Stability in Fluorine-Treated Al-Rich High Electron Transistors with 85% Al-Barrier Composition

SAND2019-1463C

Albert G. Baca, B. A. Klein, A. M. Armstrong, A. A. Allerman, E. A. Douglas, T. R. Fortune, and R. J. Kaplar

Sandia National Laboratories, PO Box 5800, Albuquerque, NM 87185-1085 USA

***Abstract*—Combined with recess etching, Al-rich III-N high electron mobility transistors (HEMTs) can be treated with a reactive ion etch plasma to implant F^- ions into the HEMT's near surface region for a positive threshold voltage (V_{TH}) shift to achieve enhancement-mode (e-mode) operation. These HEMTs, along with depletion-mode (d-mode) controls that lack fluorine treatment, were evaluated for F^- ion stability using step-stress and fixed-bias stress experiments. Step-stress experiments identified parametric shifts as a function of the drain-voltage (V_{DS}) stress prior to catastrophic failure that occurred at V_{DS} ranging between 70-75 V. Fixed bias stressing at V_{DS} = 50 V was conducted at 190°C. Both e- and d-mode HEMTs exhibited a negative V_{TH} shift of 0.6-1.0 V during early time stressing at 190°C, with minor on-resistance effects, but both HEMT types were thereafter stable up to 4 hours. The early time changes are common to both e-mode and d-mode HEMTs and the F-induced V_{TH} delta between e- and d-mode HEMTs remains intact within the bias-temperature stressing conditions of this work.**

Keywords- Al-rich AlGaN, high electron mobility transistor, HEMT, ultra-wide bandgap, UWBG, fluorine ion stability.

I. Introduction

Ultra-wide bandgap (UWBG) semiconductors are an emerging class of materials for the next generation of power and RF electronics. Al-rich AlGaN-channel devices are among those UWBG materials with the most promising figures of merit [1, 2]. The recent literature for these emerging devices is heavily weighted towards depletion-mode (d-mode) transistors [3-9], yet enhancement-mode (e-mode) transistors are necessary for power switching applications. During the development of AlGaN/GaN HEMTs, various approaches were proposed for e-mode devices, including a **F**-treatment to the gate-AlGaN interface [10]. Although doubts about the stability of threshold voltage have been raised, only a single reliability study addresses these [11] and the doubts have persisted. The recent development of **F**-treated AlGaN-channel HEMTs in our research group [12] effectively renews the question of fluorine stability. Notwithstanding any prior **F**-stability results for GaN-channel HEMTs (25% Al barrier), the topic is worth reexamining in light of the expected higher bond strength of Al-bonded F^- ions compared to Ga-bonded F^- ions and the preponderance of group III Al in $Al_{0.85}Ga_{0.15}N/Al_{0.7}Ga_{0.3}N$. A comprehensive reliability study is not usually warranted in an immature technology. However, judiciously chosen stress experiments, the subject of this paper, can shed light on the important question of F^- ion stability in Al-rich AlGaN transistors.

II. Description of Device and Stress Procedure

The epitaxial structure, grown by metal organic chemical vapor deposition on a sapphire substrate, consists of a 1.6 µm AlN buffer and nucleation layer, a 330 nm $Al_{0.7}Ga_{0.3}N$ channel layer, and a 50 nm Si-doped $Al_{0.85}Ga_{0.15}N$ barrier layer. Circular HEMTs were fabricated similarly to those described previously [12,13]. They were constructed with a 200 µm diameter drain contact, an 8 µm source-drain separation, and a 3 µm gate contact based on a Ni/Au Schottky barrier, centered between the source and drain. The Zr/Al/Mo/Au Ohmic contacts were alloyed at 1100°C and show rectifying behavior due to the high Al-content of the barrier layer. After source/drain formation, 100 nm of SiN was deposited. A 3 µm gate opening in the SiN was next formed by reactive ion etching. Long exposure to the **F**-RIE plasma leads to e-mode HEMTs from a combination of surface F^- ions and gate recessing [13] (Fig. 1). In contrast, minimal **F**-RIE plasma exposure leads to depletion-mode HEMTs with only a slight, unintentional recess [9]. After another lithography process, Ni/Au gates were deposited into the vacated SiN regions and overlapped the adjacent SiN for "field-plate" type gate-edge termination.

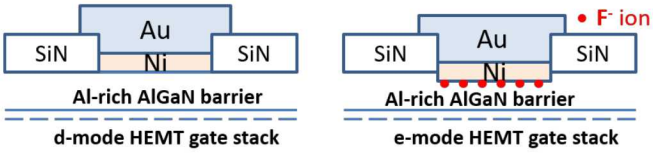

Figure 1. *Schematic cross-section of HEMT illustrating the role of F^- ion treatment in creating an e-mode transistor.*

$Al_{0.85}Ga_{0.15}N/Al_{0.7}Ga_{0.3}N$ HEMTs treated with F^- ions were verified to contain **F** atoms in the near surface regions by Auger electron spectroscopy, time-of-flight secondary ion mass spectroscopy, and V_{TH} modeling [13]. Approximately 41% of the V_{TH} shift was ascribed to F^- ions, with the rest ascribed to a 12 nm gate recess.

Both fixed-bias and step-stress experiments were performed on these devices, at room temperature and at 190°C. The step-stress experiments were performed at several gate biases (V_{GS}), as illustrated in Fig. 2. The step-stress experiments use 5 V drain voltage (V_{DS}) steps, 100 s stress intervals, continuous monitoring of source, gate, and drain currents during stress, and more substantial electrical characterization, between stress steps. The electrical characterization consisted of non-stressing voltage sweeps, recorded at designated stress interruptions, before and after each stress segment. The stress duration was fixed at 100 s for step-stress experiments, and of variable length, progressively increasing, for fixed-bias stress experiments. Different V_{GS} during separate stress experiments allows for comparison of low, moderate, and high levels of hot electrons to evaluate **F**-stability under all of these conditions. Fig. 2 was generated to describe an e-mode HEMT stress experiment. The V_{GS} = -2 V bias condition leads to HEMT pinch-off, with leakage current as the source of hot electrons. The corresponding d-mode HEMTs bias condition is V_{GS} = -10 V. Trends based on electrical parameters were tracked against stress time and magnitude. V_{DS} step-stressing enables the rapid identification of important stress conditions as well as identification of the destructive V_{DS}.

III. Data/Results and Discussion

At least two types of effects are important for the stress experiments employed in this study, namely, hot electrons from large V_{DS} electric fields and the response of F^- ions to the electric

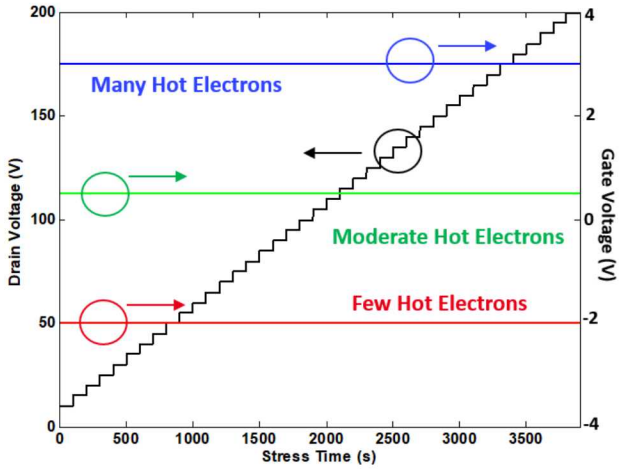

Figure 2. E-mode HEMT *step-stress experimental design using stepped drain voltage at a fixed gate voltage (several) to vary the incidence of hot electrons.*

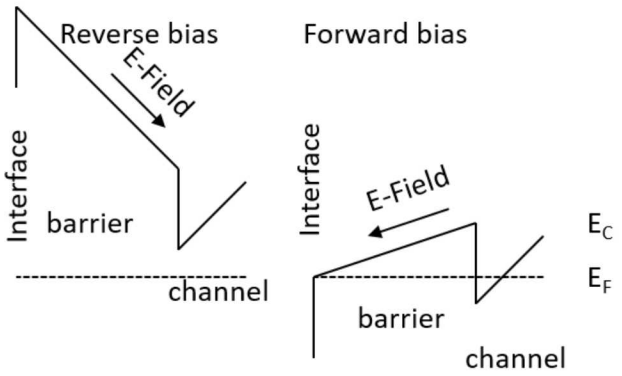

Figure 3. *The electric field of the AlGaN barrier may act on electrons to drive them away from the HEMT interface in reverse bias, but not in forward bias.*

field applied across the barrier. The hot electron density differs by more than 6 orders of magnitude, depending on the gate bias. Hot electrons arising from lateral (parallel to the surface) electric field stress can be expected to affect both d-mode and e-mode HEMTs similarly. However, vertical (perpendicular to the surface) electric field stress may affect the mobility of $\mathbf{F}^-$ ions in e-mode HEMTs, particularly in combination with any thermal stress. Specifically, the magnitude of the electric field from the gate bias can drive $\mathbf{F}^-$ ions towards or away from the AlGaN interface with Ni, depending on the gate bias, as illustrated notionally in Fig. 3. In reverse bias, the gate bias provides a force for possible drift away from the Ni-AlGaN interface, while forward bias provides a force for possible drift towards the Ni-AlGaN interface. The intermediate bias condition with V_{GS} = + 0.5 V provides a lesser magnitude of vertical electric field.

The results of e-mode HEMT step-stress experiments under bias conditions representing low, moderate, and high densities of hot electrons are illustrated in Fig. 4 for I_D vs. stress time (also vs. V_{DS}). Source current tracked similarly but was opposite in polarity. Gate current was very small and largely inconsequential. At modest V_{DS} stress, the off-state drain current (I_D) is < 10^{-6} mA for V_{GS} = -2 V, I_D ~ 10^{-2} mA for V_{GS} = +0.5 V, and I_D ~ 5-6 mA for V_{GS} = +3 V. Under reverse bias stressing (V_{GS} = -2 V), I_D increases exponentially with V_{DS} stress and also during the individual V_{DS} stress intervals. This latter effect is illustrated in the inset to Fig. 4 and is evidence of trapping/de-

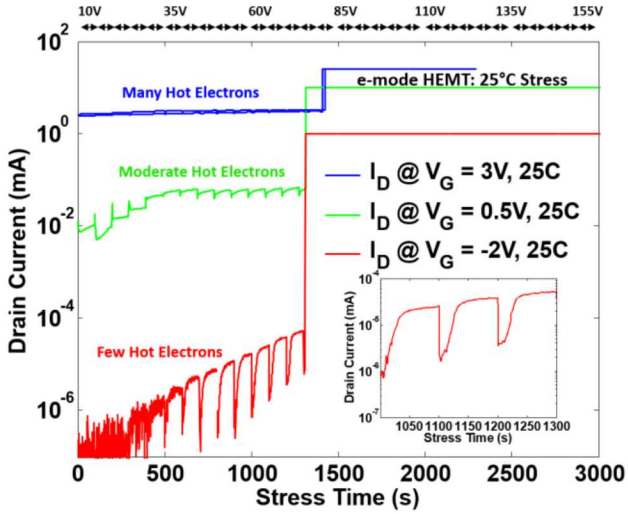

Figure 4. *Evolution of drain current vs. stress time in e-mode Al-rich HEMTs at 25°C as V_{DS}, shown at the top of the plot, is stepped from 10-155V, for low, moderate, and many hot electrons.*

trapping behavior, whereby I_D is < 10^{-6} mA at the onset of the 1000 s stress interval and exponentially rises to > 10^{-5} mA by 1030 s, whereupon the I_D rise is slower. Electron de-trapping during a stress cycle accounts for the I_D increase. Then electron trapping during the subsequent parametric characterization that uses lower, non-stressing V_{DS} accounts for I_D that is reset to a lower level at the initiation of the next stress cycle. As the process repeats, both peak and trough I_D increase in each subsequent cycle. The trapping/de-trapping behavior of the inset to Fig. 4 is similar to the stress/recovery experiments described by del Alamo and Joh [14]. It applies to the case of "few hot electrons" and also may apply to a lesser degree for "moderate hot electrons." If present in the case of "many hot electrons," its relative magnitude may be less or it may occur over a much shorter or longer time window than is apparent from Fig. 4. These effects deserve further scrutiny, but are beyond the scope of this paper. The differing densities of hot electrons are associated with destructive voltages of 70-75 V. The similarity in destructive voltages seems to indicate that hot electron density is secondary in importance to the lateral electric field for destructive degradation of e-mode HEMTs.

Figs. 5 and 6 illustrate the progression of I_D-V_{DS} and I_D-V_{GS} plots, respectively, for stress experiments conducted with reverse biased gates and V_{DS} stepped from 10 V to 70 V (blue to red in the direction of the arrow). The d-mode HEMTs show decreasing I_D in Fig. 5(a), while the e-mode HEMTs show increasing I_D in Fig. 5(b). On-resistance degradation is

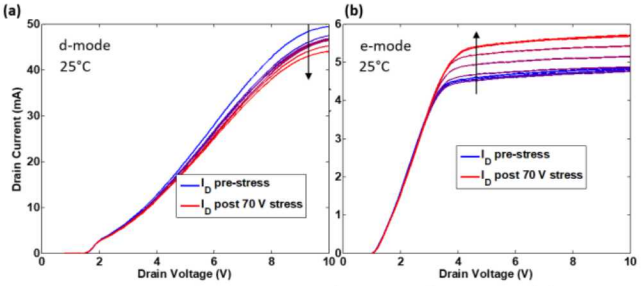

Figure 5. 25°C progression I_D-V_{DS} *plots (at V_{GS} = 4V) in d-mode (a) and e-mode (b) HEMT step-stress experiments (d-mode stress: V_{GS}= -10 V, e-mode stress: V_{GS} = -2V). I_{MAX} changes in opposite directions for e-mode and d-mode HEMTs subjected to reverse bias stress.*

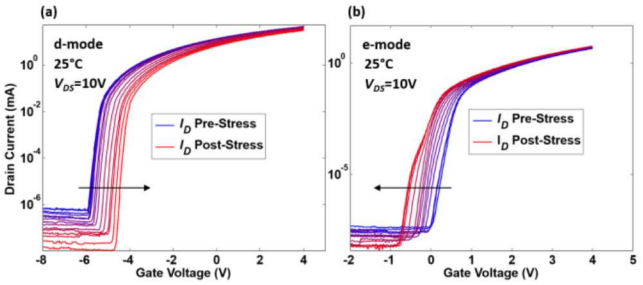

Figure 6. 25°C progression of I_D-V_{GS} plots in d-mode (a) and e-mode (b) HEMT step-stress experiments (d-mode stress: V_{GS}= -10 V, e-mode stress: V_{GS} = -2V). V_{TH} changes in in opposite directions for e-mode and d-mode HEMTs.

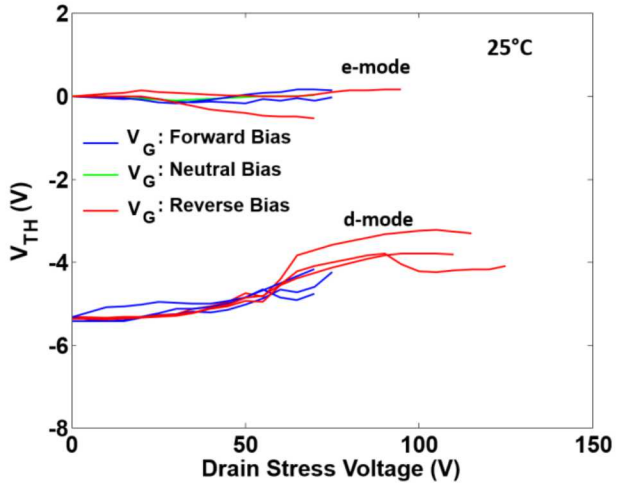

Figure 7. V_{TH} shift vs. V_{DS} stress for d- and e-mode HEMTs stressed at 25°C and V_{GS} = +3 V (forward bias), +0.5 V or -2 V (e- and d-mode neutral bias), -2 V (reverse bias, e-mode), or -10 V (reverse biase, d-mode).

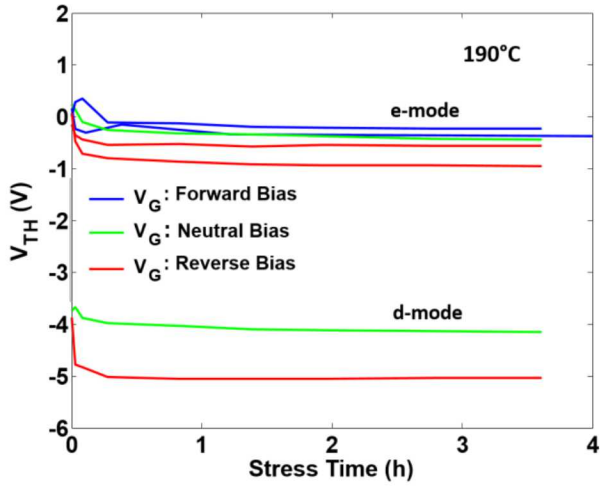

Figure 8. V_{TH} stability measured during stress interruptions for e-mode and d-mode HEMTs stressed at 190°C under forward (V_{GS} = +3 V), neutral (V_{GS} = +0.5 V for e-mode and V_{GS} = -2 V for d-mode) and reverse (V_{GS} = -2 V for e-mode and V_{GS} = -10 V for d-mode) bias all with V_{DS} = 50 V.

negligible for the e-mode HEMTs and only slight for d-mode HEMTs undergoing reverse bias stress. Fig. 6 illustrates that the origin of the I_D shifts of Fig. 5 are from V_{TH} shifts, positive for d-mode HEMTs, and negative for e-mode. The V_{TH} shift for e-mode HEMTs only applies to the reverse bias and is much reduced for gates under neutral (defined as V_{GS} = 0.5 V for e-mode HEMTs and V_{GS} = -2 V for d-mode HEMTs, to fulfill the intent of "moderate" hot electrons) or forward bias, as seen in Fig. 7. Understanding the V_{TH} trends for reverse bias stressing will require further investigation, but may not be consequential for e-mode devices not operated in reverse bias.

The aforementioned room temperature step-stress experiments enable the judicious choice of bias conditions for stressing at elevated temperature. Based on devices stressed in the manner of Fig. 4, a V_{DS} = 50 V stress condition was chosen for subsequent 190°C stressing. The 190°C stress experiments were carried out with stress interruptions at 100, 300, 1000, 3000, 7000, 10000, and 13000 s, where stress interruptions at those times allowed parametric characterization at 190°C. Since the HEMT's parametric values change very little over the 0-200°C temperature range [12], they are a good proxy for the room temperature values. Fig. 8 illustrates the trend in V_{TH} for both e- and d-mode HEMTs. An early time shift in V_{TH} is observed for all stress conditions but is one that stabilizes by 1000 s (0.28 h). The magnitude of the shift is greatest for HEMTs that are stressed under reverse bias, ~1.2 V for d-mode and 0.6-1.0 V for e-mode HEMTs. For HEMTs stressed under neutral or forward bias, the magnitude of the V_{TH} shift is modest, ~ 0.2-0.7 V, and the early time trend is not always to more negative V_{TH}.

Fig. 9 illustrates the trends from one of the e-mode HEMTs for the I_D-V_{GS} plots captured during 190°C stress interruptions. Rapid changes occur during the first two stress intervals, but only slight changes occur after 0.28 h. I_D at V_{GS} = 4 V is increasing, similar to Figs. 5-6. In Fig. 9, all of the curves shift to the left in a parallel manner, as observed in the subthreshold region. Consistent subthreshold slope and consistently low leakage currents with high on/off ratio at elevated temperature are consistent with a HEMT lacking intrinsic degradation during the 3.6 h stress. These observations support the earlier assertions that non-permanent trapping/de-trapping behavior may be responsible for the V_{TH} shifts.

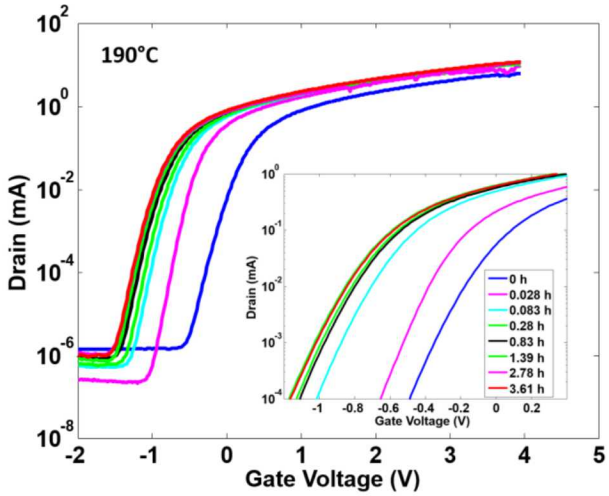

Figure 9. Progression of I_D-V_{GS} plots over 3.61 h of stress for e-mode HEMTs undergoing 190°C stress at V_{GS} = -2V and V_{DS} = 50V.

In this work, we are addressing the question of $\mathbf{F}^-$ ion stability. While the data of Figs. 6-7 show that V_{TH} appears to lack stability at high enough drain stress, the data of Fig. 4 shows that repeated stress/recovery effects are an important confounding factor and such effects aren't necessarily permanent. These effects are deserving of further study with appropriate consideration to details involving the actual

conditions of an application. From the data presented here, we can address the question of $\mathbf{F}^-$ ion stability resulting from stress involving a constant electric field profile. Since the V_{TH} shift affects both d-mode and e-mode HEMTs similarly in Fig. 8, it is presumed to have a common cause for both. Since only the e-mode HEMTs were intentionally treated with $\mathbf{F}^-$ ions, it follows that that $\mathbf{F}^-$ ions are not the cause of the shift. In fact, the lack of large differences in stress response between d-mode and e-mode HEMTs can be construed as evidence $\mathbf{F}^-$ ions are stable at 190°C, with the caveat that a slight early time $\mathbf{F}^-$ ion instability may be masked by the larger common instability. The early time negative V_{TH} shift is still potentially detrimental regardless of its origin. A possible remediation, may involve targeting the initial V_{TH} more positively by means of a longer **F**-exposure.

A similar analysis to that used in ref. [13] quantifies the effect of the $\mathbf{F}^-$ ions on V_{TH} of the e-mode HEMT and also supports the assertion of its stability. The HEMTs show a consistent delta of $V_{TH} \sim 4$ V between the e-mode and the d-mode HEMTs. Two factors account for the V_{TH} delta: recess etch depth, accounting for 59%, or 2.4 V of the shift, and $\mathbf{F}^-$ ions, which account for approximately 41% or ~1.6 V of the shift. A change in Schottky barrier height could affect V_{TH}, but would likely affect a d-mode HEMT equally. Lacking a reason to suspect recess etch instability, we arrive at a similar conclusion: $\mathbf{F}^-$ ions remain intact to influence V_{TH} similarly before and after 190°C stressing. Even so, important details relating to $\mathbf{F}^-$ ion stability may be incomplete and further investigation is warranted. A second important consideration for e-mode HEMTs is that for power conversion applications the neutral and forward bias conditions will be of greater importance than the reverse biased stress, resulting in less consequence to the early time V_{TH} stabilization, except to note that V_{TH} targeting to more positive V_{TH} is needed.

Beyond the question of $\mathbf{F}^-$ ion stability under various bias conditions, a tentative picture of hot electron behavior can be summarized as follows. Hot electron stress is associated with temporal trapping/de-trapping behavior that appears to have a considerable partial recovery of I_D that approaches prior values. This type of behavior displays commonality to similar types of stress/recovery effects in AlGaN/GaN HEMTs [14]. However, high electric fields, rather than hot electron stress, leads to HEMT destruction, at similar drain voltages regardless of gate bias or hot electron density (Fig. 4). The d-mode HEMTs were more robust to electric field stress and displayed higher and more variable destructive voltages, as seen in Fig. 7. Factors other than hot electrons are important in the destructive failure mechanism, and further investigation is warranted.

IV. Conclusions

This work presents evidence that $\mathbf{F}^-$ ions appear to not be vulnerable to V_{TH} instability when stressed up to 4 hours at 190°C and V_{DS} = 50 V in Al-rich e-mode HEMTs. However, a common V_{TH} shift affects both e- and d-mode HEMTs at early times followed by relatively stable behavior. The similarity in destructive voltages of 70-75 V seems to indicate that hot electron density is secondary in importance to the lateral electric field for destructive degradation of e-mode HEMTs. Future work will need to account for trapping/de-trapping effects in order to build a more complete understanding of Al-rich HEMT degradation.

V. Acknowledgments

This work was supported by the Laboratory Directed Research and Development program at Sandia National Laboratories. Sandia National Laboratories is a multi-program laboratory managed and operated by National Technology & Engineering Solutions of Sandia, LLC (NTESS), a wholly owned subsidiary of Honeywell Corporation, for the U.S. Department of Energy's National Nuclear Security Administration under contract DE-NA0003525. The views expressed in the article do not necessarily represent the views of the U.S. Department of Energy or the United States Government.

References

[1] R. J. Kaplar, A. A. Allerman, A. M. Armstrong, M. H. Crawford, J. R. Dickerson, A. J. Fischer, A. G. Baca, and E. A. Douglas, "Review—Ultra-Wide-Bandgap AlGaN Power Electronic Devices," *ECS J. Solid State Science and Technology*, vol. 6, pp. Q3061- Q3066 (2017).

[2] M. E. Coltrin, A. G. Baca, and R. J. Kaplar, "Analysis of 2D Transport and Performance Characteristics for Lateral Power Devices Based on AlGaN Alloys", *ECS J. Solid State Science and Technology,* vol. 6, pp. S3114-18 (2017).

[3] N. Yafune, S. Hashimoto, K. Akita, Y. Yamamoto, H. Tokuda and M. Kuzuhara, "AlN/AlGaN HEMTs on AlN substrate for stable high-temperature operation," Electron. Lett. vol. 50, pp. 211-212 (2014).

[4] S. Bajaj, F. Akyol, S. Krishnamoorthy, Y. Zhang, and S. Rajan, "AlGaN channel field effect transistors with graded heterostructure ohmic contacts," *Appl. Phys. Lett.,* vol. 109, pp. 133508-133511 (2016).

[5] A. G. Baca, A. M. Armstrong, A. A. Allerman, E. A. Douglas, C. A. Sanchez, M. P. King, M. E. Coltrin, T. R. Fortune, and R. J. Kaplar, "An AlN/$Al_{0.85}Ga_{0.15}N$ high electron mobility transistor," *Appl. Phys. Lett.* vol. 109, pp. 033509-033512 (2016).

[6] S. Muhtadi, S. M. Hwang, A. Coleman, F. Asif, G. Simin, M. V. S. Chandrashekhar, and A. Khan, "High Electron Mobility Transistors With $Al_{0.65}Ga_{0.35}N$ Channel Layers on Thick AlN/Sapphire Templates," *IEEE Electron Dev. Lett.,* vol. 38, pp. 914-917 (2017).

[7] S. Bajaj, A. Allerman, A. Armstrong, T. Razzak, V. Talesara, W. Sun, S. H. Sohel, Y. Zhang, W. Lu, A. R. Arehart, F. Akyol, and S. Rajan, "High Al-content AlGaN Transistor With 0.5 A/mm Current Density and Lateral Breakdown Field Exceeding 3.6 MV/cm, *IEEE Elec. Dev. Lett.* vol. 39, pp. 256-259 (2018).

[8] A. M. Armstrong, B. A. Klein, A. Colon, A. A. Allerman, E. A. Douglas, A. G. Baca, T. R. Fortune, V. M. Abate, S. Bajaj, and S. Rajan, "Ultra-wide band gap AlGaN polarization-doped field effect transistor," *Jap. J. Appl. Phys.* vol. 57, pp. 074103-1-074103-5 (2018).

[9] A. G. Baca B. A. Klein, J. R. Wendt, S. M. Lepkowski, C. D. Nordquist, A. M. Armstrong, A. A. Allerman, E. A. Douglas, and R. J. Kaplar, "RF Performance of $Al_{0.85}Ga_{0.15}N/Al_{0.70}Ga_{0.30}N$ High Electron Mobility Transistors With 80 nm Gates," *IEEE Electron Device Letters*, vol. 40, pp. 17-20 (2019).

[10] Y. Cai, Y. Zhou, K. M. Lau, and K. J. Chen, "Control of Threshold Voltage of AlGaN/GaN HEMTs by Fluoride-Based Plasma Treatment: From Depletion Mode to Enhancement Mode," *IEEE Transactions on Electron Devices,* vol. 53, pp. 2207-2215, 2006.

[11] C. Yi, R. Wang, W. Huang, W. C. -W. Tang, K. M. Lau, and K. J. Chen, "Reliability of Enhancement-mode AlGaN/GaN HEMTs Fabricated by Fluorine Plasma Treatment," *Proc. Int. Electron Device Meeting*, pp. 389-392 (2007).

[12] A. G. Baca , B. A. Klein, A. A. Allerman, A. M. Armstrong, E. A. Douglas, C. A. Stephenson, T. R. Fortune, and R. J. Kaplar, "$Al_{0.85}Ga_{0.15}N/Al_{0.70}Ga_{0.30}N$ High Electron Mobility Transistors with Schottky Gates and Large On/Off Current Ratio over Temperature," *ECS J. Solid State Science and Technology*, vol. 6, pp. Q161-Q165 (2017).

[13] B. A. Klein, E. A. Douglas, A. M. Armstrong, A. A. Allerman, V. M. Abate,T. R. Fortune, and A. G. Baca, "Enhancement-Mode $Al_{0.85}Ga_{0.15}N/Al_{0.7}Ga_{0.3}N$ High Electron Mobility Transistor with Fluorine Treatment,"submitted to *Appl. Phus. Lett.*

[14] J. A. del Alamo and J. Joh, "GaN HEMT Reliability," *Microelectronics Reliability,* vol. 49, pp. 1200-1206 (2009).